International Journal of GEOMATE, June 2019, Vol.16, Issue 58, pp.55 - 61
Geotec., Const. Mat. & Env., DOI: https://doi.org/10.21660/2019.58.8139
ISSN: 2186-2982 (Print), 2186-2990 (Online), Japan

INVESTIGATION OF THE FLEXURAL STRENGTH OF COLD-FORMED STEEL C-SECTIONS USING COMPUTATIONAL AND EXPERIMENTAL METHOD

Bernardo A. Lejano[1] and Eyen James D. Ledesma[2]

[1,2] Gokongwei College of Engineering, De La Salle University, Philippines

*Corresponding Author, Received: 24 Oct. 2018, Revised: 27 Dec. 2018, Accepted: 10 Jan. 2019

ABSTRACT: Cold-formed steel (CFS) as a structural material has gained popularity because of its high strength-to-weight ratio. In the Philippines, the demand to use it as the structural member has increased recently. However, verification of its actual strength is not extensively studied in the country. To conform to the design standards of the local code, the National Structural Code of the Philippines (NSCP), CFS as a structural member are required to be ductile. However, it was discovered that CFS with higher strength but with brittle behavior is also being commercially distributed in the country. The objective of this study is to investigate the flexural strength of CFS made of these steel materials with the use of the computational and experimental method. The computational method covers the calculation of the theoretical flexural strength based on the NSCP provisions while the experimental method covers the actual flexural strength based on the four-point bend test. A total of 24 specimens of back-to-back C-sections of different thicknesses and lengths were tested. Additional finite element method (FEM) calculation was also conducted using ANSYS. The main failure modes were distortional buckling (DB) and lateral-torsional buckling (LTB). For the ductile CFS, DB and LTB were observed in 86.1% and 13.9% of specimen population, respectively. While for the brittle CFS, DB and LTB were observed in 75.0% and 25.0%, respectively. Moreover, it was found that the computational strengths were lower than the experimental strengths. The FEM analysis results were close to the experimental results thus validating the experimental results.

Keywords: Cold-formed Steel, C-section, Four-Point Bend Test, ANSYS, NSCP

1. INTRODUCTION

There are two types of steel mostly used in the construction industry: hot-rolled steel and cold-formed steel (CFS). CFS is composed of flat sheets and strips of metal shaped by either rolling or pressing. It can be produced economically by the cold-forming process, and favorable strength-to-weight ratios can be obtained [1]. Figure 1 shows the typical configuration of a CFS C-section.

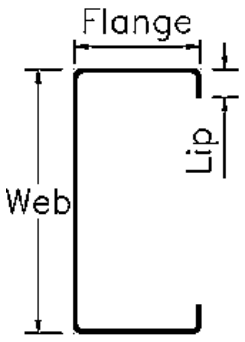

Fig.1 Typical configuration of CFS C-section

In the Philippines, CFS is locally produced and manufactured. But foreign standards have been adopted ever since its use and application in the country. CFS is not extensively studied in the country and its design is based on foreign standards, mostly based on the American Iron and Steel Institute (AISI), as specified in the National Structural Code of the Philippines (NSCP) [2]. It is a practice that if the code is simply followed then the design work is acceptable. To conform to the design provisions, CFS as a structural member is required to be typically ductile. However, it was discovered that CFS with higher strength but with brittle behavior is also being commercially distributed in the country. Whether ductile or brittle, the actual performance of locally distributed CFS needs to be investigated if their actual strength is consistent with the theoretical strength based on the NSCP. Previous studies have already reported inconsistencies in the computation of the concentric compressive strength of C-section and Z-section based on NSCP as compared to experimental values [3], [4]. In line with this, the aim of this study is to investigate the actual flexural strength of CFS C-sections made of both ductile and brittle steel materials and compare this with the values obtained from computational (based on NSCP) and numerical method (based on finite element analysis).

2. METHODOLOGY

This study covers both computational and experimental method. The computational method covers the calculation of the theoretical flexural strength based on the NSCP provisions for CFS while the experimental method covers the actual flexural strength based on the four-point bend test conducted for each steel material. Additional analysis and comparison were also done using the finite element analysis software, ANSYS. This helped in further analyzing the accuracy of the results of the two methods for both types of steel.

2.1 CFS C-Section Specimens

The C-section used in the study is defined as a singly-symmetric section. The section size of the specimens used conforms to the dimensional limits specified in NSCP Section 553.3. A 50 mm (flange) x 100 mm (web) C-section with lip stiffeners was used in the study since this is the most commonly used section in the industry. The section used has lips which act as edge stiffener to the flanges but has no intermediate stiffeners along the web of the member. Three lengths and two thicknesses were used for both ductile steel (DS) and brittle steel (BS). Three trials were considered for the ductile CFS, while only one trial for the brittle CFS, for a total of 24 back-to-back CFS C-section (48 individual CFS) tested in this study; 18 DS and 6 BS.

The lengths used for the specimens were limited due to the space that can be accommodated in the testing lab. The thicknesses were based on the commercial availability of the members. A digital Vernier caliper was used to measure the actual dimensions of the specimens to assure accurate calculations. Table 1 shows the specimen codes used in the study.

Table 1 Specimen codes used

Code	Steel Type	Length (mm)	Thickness (mm)
A1	DS	1000	2.0
A2	DS	2000	2.0
A3	DS	3000	2.0
B1	DS	1000	1.2
B2	DS	2000	1.2
B3	DS	3000	1.2
C1	BS	1000	2.0
C2	BS	2000	2.0
C3	BS	3000	2.0
D1	BS	1000	1.2
D2	BS	2000	1.2
D3	BS	3000	1.2

For example, code A1 refers to C-section CFS with ductile steel material with 1000 mm length and 2 mm thickness.

Material properties were determined following the procedure from ASTM E8 (Standard Test Methods for Tension Testing of Metallic Materials) [5]. Metal strips conforming to the standard of ASTM E8 were cut and tested in tension to determine the actual yield strength and modulus of elasticity of both steel materials. The load-strain curves were also plotted so that the behavior of the CFS can be visualized. These properties, along with the actual dimensions of the specimens, were used in computing for the theoretical flexural strength of the members based on NSCP.

2.2 Experimental Setup of the Four-Point Bend Test

The schematic drawing and actual setup of the four-point bend test used in the study are shown in Figure 2 and 3, respectively. The end supports for the test were simply supported, with the applied loads passing through the centroid of the back-to-back channels. The load was applied using a hydraulic jack and monitored using a load cell. The adopted experimental setup for the study was mostly based on the experimental setup used by Wang and Young [6], which also cover CFS sections subjected to bending.

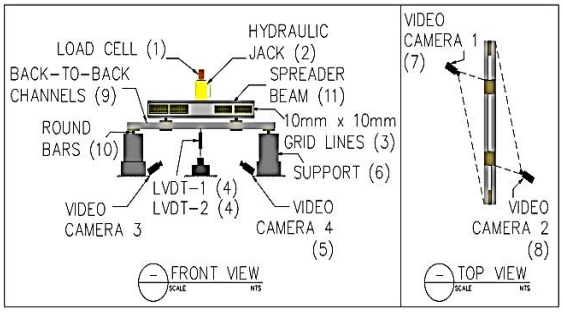

Fig.2 Schematic drawing of the four-point bend test

Fig.3 Actual setup of the four-point bend test

Based on the experimental setup, two channels bolted back-to-back were tested at the same time to avoid out-of-plane bending of the member. These channels were bolted to T-shaped wooden blocks. They are placed at the end supports and at the loading points to act as stiffeners to the web of the member in order to prevent crippling and sudden failure at those points.

Two displacement transducers (LVDT 1 and 2) were placed at the middle of the moment span under each specimen in order to record its vertical displacement. The entire experimental test was captured and recorded using four high-speed video cameras to precisely evaluate the buckling failure modes manifested by each member. Gridlines, 10 mm x 10 mm, were placed along the length of the member to help in scaling the movement of its elements.

In addition, two round high-tempered steel bars were used to act as simple supports in the test setup. For the spacing of the back-to-back channels, the distance of each channel from its outer web fiber was established approximately as twice the average shear center for one channel. In theory, setting this spacing makes the line of action of the applied load pass not only to the centroid and shear center of the back-to-back channel but also to the shear center of one channel. This avoids complication of the application of torsion in the section.

2.3 Failure Modes

The main modes of failure for CFS members in flexure as listed in the NSCP are yielding, distortional buckling (DB) and lateral-torsional buckling (LTB). However, only DB and LTB were manifested by the specimens in the experiment.

For DB, its mode shape involves both rotation and translation of the fold lines of the member. It is relatively a new type of failure mode in a sense that current design specifications do not have sufficient procedure for design against distortional buckling [7]. However, many types of research and experimental tests have already been completed to predict DB in CFS members. One study says that this type of buckling is the controlling failure mode for most CFS sections with deep and slender webs [8]. For the C-section used, DB occurs because of the edge stiffened flanges present in the section. It is due to the instability of the flange that causes the flange, along with the edge stiffener, to rotate about the flange-web junction.

For LTB, its mode shape involves either both translation and rotation of the entire cross-section. CFS members are susceptible to LTB because of the geometry of its section, particularly open sections such as C-section. This is because CFS open sections give great flexural rigidity about one axis at the expense of low torsional rigidity about the perpendicular axis [9].

Most of the time, local buckling triggers the movement of failure modes. It is not listed as a mode of failure in the NSCP but was considered as a factor to the strength of the member by using its effective area. Figure 4 shows the different modes of failure that can be exhibited by a member loaded in flexure. Movement of the elements shown can vary and show a more complex configuration. It is important to note that multiple modes of failure can be manifested by a member simultaneously.

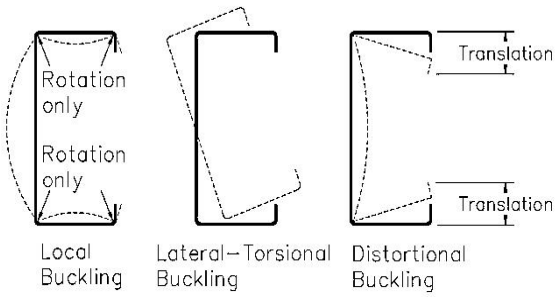

Fig.4 Failure modes for C-section CFS flexural members

3. RESULTS AND DISCUSSION

Two steel materials, namely ductile and brittle steel, were investigated in the study for the CFS members. The tensile test results attained for the material properties of the members were based on ASTM E8 [5]. For the ductile and brittle CFS, the average yield strength obtained using ASTM E8 was 265.27 MPa and 561.82 MPa, respectively, while the average modulus of elasticity was 39.09 GPa and 58.49 GPa, respectively.

It was observed from the tension testing that the ductile CFS clearly exhibited yielding plateau after the elastic stage was exceeded. On the other hand, the brittle CFS exhibited a sudden drop in strength after reaching the yielding stress.

3.1 Experimental Flexural Strength

Since back-to-back channels were tested simultaneously in the four-point bend test, the actual flexural strength for each specimen was taken as the maximum load recorded from the load cell divided by two. This is termed as the experimental strength. It was used instead of the flexural moment for better comparison of the results attained in the experiment. In addition, the self-weight of the member, weights of the T-shaped wooden blocks, round bars at the loading points, hydraulic jack and spreader beam were all accounted for in computing the experimental

strength for each member. Table 2 shows the average experimental strength for all trials of the specimen.

Table 2 Experimental strengths (kN)

Code	1	2	3
A	38.69	17.53	10.59
B	19.70	9.69	6.93
C	44.45	28.47	12.71
D	26.43	12.96	7.17

Based on the experimental strengths shown in Table 2, it can be observed that the strength of the member is affected by both its length and thickness. Shorter length members attained larger strengths than the longer ones. The length mostly influenced the type of failure mode for the member in terms of its global buckling while the thickness influenced the local buckling response of the members.

Relating the difference of the corresponding results for the ductile and brittle CFS, it is also observed that the strengths attained for the longer lengths by the ductile CFS were marginally lower than the brittle CFS. However, for the shorter lengths, it is comparatively higher. Hence, the substantial difference between both steel materials' yield strength only had a minimal effect on their experimental strengths for the longer lengths, but for the shorter lengths, it had a sizeable difference.

DB and LTB were the main failure modes manifested in the experiment. Figure 5 and 6 show an example for both DB and LTB failure observed in the experiment.

Fig.5 Distortional buckling failure

Fig.6 Lateral-torsional buckling failure

3.2 Computational Flexural Strength

The computational strengths of the specimens were computed using the design provisions of the NSCP for CFS, which can be found in Section 552 and 553 of the code. Yielding, DB and LTB are the main failure modes specified in the NSCP for CFS flexural members. The governing strength was taken as the lowest moment computed amongst the three. Table 3 summarizes the average computational strengths for all trials.

Table 3 Computational strengths (kN)

Code	1	2	3
A	22.90	12.40	7.77
B	11.37	5.27	3.73
C	49.49	18.56	12.85
D	20.46	10.12	4.30

The same observation as that of the experimental results can be said for the computational results shown in Table 3, though it can be observed that the strengths attained by the ductile CFS were comparatively lower than the brittle CFS for all lengths and thicknesses. In addition, only DB was calculated as the governing failure mode for all the computational strengths.

3.3 FEM Flexural Strength

The FEM strengths were determined by generating the model for each specimen and simulating it using ANSYS. The gathered results were used to further compare and analyze the results from the computational and experimental method.

Models for each specimen were generated by using their actual dimensions and properties. Measured densities of 7786 kg/m^3 and 7185 kg/m^3 were used for the ductile and brittle CFS, respectively. Boundary conditions were also set to simulate the actual supports used in the experiment. Table 4 shows the average FEM strengths for all trials generated by the software.

Table 4 FEM strengths (kN)

Code	1	2	3
A	28.04	29.59	17.14
B	15.76	5.87	5.32
C	50.92	31.81	21.45
D	23.77	9.83	4.47

A unit load for the two loading points was used as the initial load for the FEM. Dummy plates were modeled to transfer the unit load to the shear center. Eigenvalue buckling analysis in ANSYS was used to simulate the buckling modes [10]. Figure 7 illustrates the failure mode for specimen B1. The strength is equal to the load multiplier multiplied by two (due to two loading points), with the units in Newton.

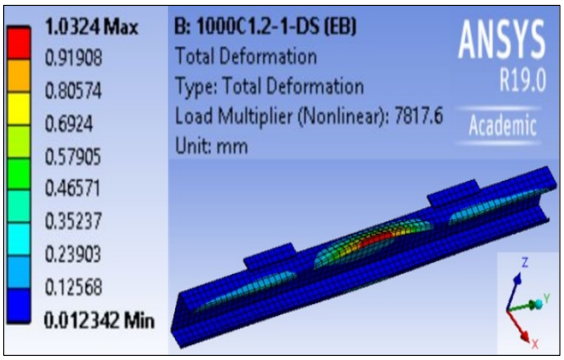

Fig.7 Buckling-failure of specimen B1 in ANSYS

3.4 Evaluation of flexural strength results

Determining the failure mode is important in the evaluation of the strength of CFS. The results indicate that the majority of specimen population has similar failure mode observed in the experiment and obtained in computation. For the ductile CFS, 86.1% of the computed failure modes agreed with the experiment results, while for the brittle CFS, a value of 75.0% was obtained.

A summary and comparison of the strengths and failure modes are shown in Table 5. In the computational method, only DB failure was attained. This may be because the section is an open section making it prone to distortional deformation. However, in the experimental tests, although most exhibited DB failure, LTB failure was observed when the length of the specimen became longer. This resulted in 86.1% that failed in DB and 13.9% in LTB for ductile CFS. In the case of brittle CFS, 75.0% failed in DB while 25.0% in LTB.

Table 5 Failure modes and strengths summary

Code	Comp Fail.	Expt Fail.	Expt (kN)	Expt / Comp	Expt / FEM
A1	DB	DB	38.69	1.70	1.40
A2	DB	DB	17.53	1.43	0.60
A3	DB	LTB	10.59	1.37	0.62
B1	DB	DB	19.70	1.74	1.26
B2	DB	DB	9.69	1.85	1.71
B3	DB	LTB	6.93	1.86	1.31
C1	DB	DB	44.45	0.90	0.89
C2	DB	DB	28.47	1.55	0.91
C3	DB	LTB	12.71	0.99	0.59
D1	DB	DB	26.43	1.29	1.11
D2	DB	DB	12.96	1.30	1.39
D3	DB	DB	7.17	1.71	1.66

To have a better comparison between the experimental strength and the computational strength, the ratio between the two (Expt/Comp) is calculated and tabulated in Table 5. The ratio of experimental strength with respect to FEM strength (Expt/FEM) is also tabulated. Ratios greater than 1.0 mean conservative predictions. It can be seen that generally the computed values, as well as FEM values, are conservative. For ductile CFS, the average Expt/Comp ratio is 1.66, while the average Expt/FEM ratio is 1.15. It means that experimental values are closer to the FEM than the computational. On the other hand, for the brittle CFS, the difference between the average ratio of FEM and computed data points to the experimental (1.09 and 1.29, respectively) was marginally lower compared to the ductile CFS.

Figure 8 and 9 shows the comparison of the strengths, by plotting the experiment values against the computed or FEM strength values.

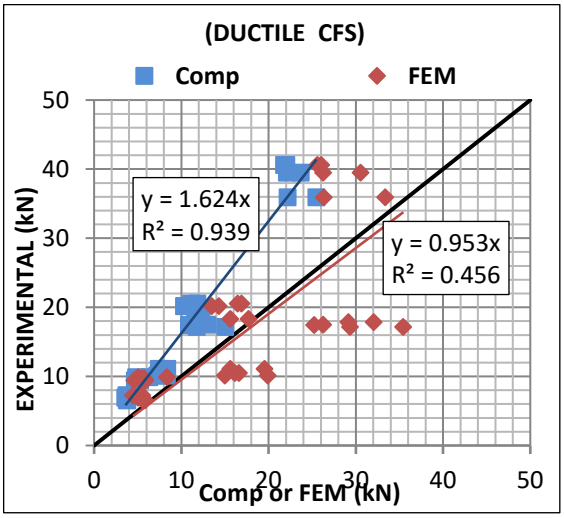

Fig.8 Strengths comparison (Ductile CFS)

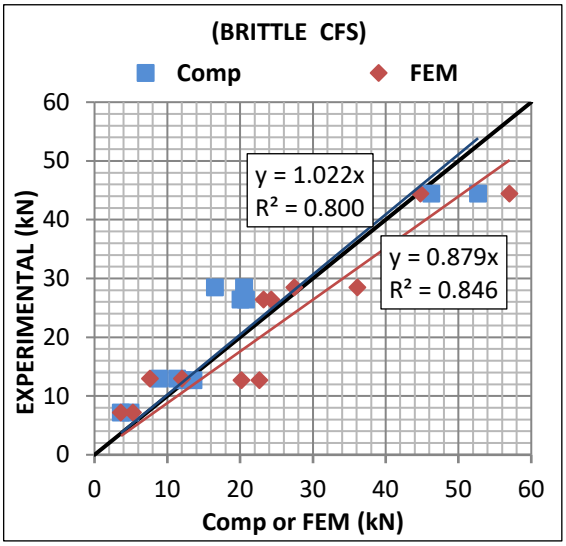

Fig.9 Strengths comparison (Brittle CFS)

The diagonal line in the graphs is the equality line. It represents points in which the computational equal to the actual (experimental). The diagonal line also represents points in which the FEM equal to the experimental.

For both steel types, the graph shows the regression line along with its corresponding correlation coefficient (R^2). It can be seen that the values R^2 are close to 1.0 indicating a good fit of the data to the regression line. Based on the graphs, the R^2 of ductile CFS for computational strength (0.939) shows a better fit than FEM (0.456). On the other hand, for the brittle CFS, its R^2 values for the computation and FEM results (0.800 and 0.846, respectively) only show marginal difference.

For the ductile CFS, the regression line of the computational data points falls above the equality line, which indicates that it is conservative (see Fig. 8). On the other hand, for the brittle CFS, the regression line of the computational data points is almost coinciding with equality line (see Fig. 9). Hence, the ductile CFS is more conservative than the brittle CFS. It may be said that the ductile CFS has a factor of safety of 1.624 based on the slope of the regression line.

The regression lines of the FEM data points of both ductile and brittle CFS are below but very close to the equality line. Thus, the FEM seems to overestimate the strength (hence nonconservative), but only by a small amount. The brittle CFS is more nonconservative than the ductile CFS.

Based on the foregoing statements, the computational strength of the ductile CFS may be applied with a modification factor to bring it close to the experimental (actual) strength. However, the other thought is that the ductile CFS is already conservative, and modifying it may pose danger. So the other alternative is to bring the brittle CFS to a conservative estimate similar to the ductile CFS. This is more appealing to safeguard against abrupt failure of brittle material. To do this, the computational strengths of the brittle CFS will be applied with a modification factor instead. The computational strength of the brittle CFS may be adjusted by multiplying it with 0.60. This value was obtained by considering that the average Expt/Comp is 1.66 for ductile CFS. Since the regression line of the computational strength of the brittle CFS almost coincides with the equality line, the modification factor can be obtained by simply taking the reciprocal of 1.66 which is equal to 0.60. After applying the modification factor, the resulting regression line is shown in Fig. 10.

Figure 10 illustrates the modified strengths for the brittle CFS. The red data points and line represent the adjusted strengths. Now, it is almost coinciding with the ductile CFS, hence, it has almost the same factor of safety as that of the ductile CFS.

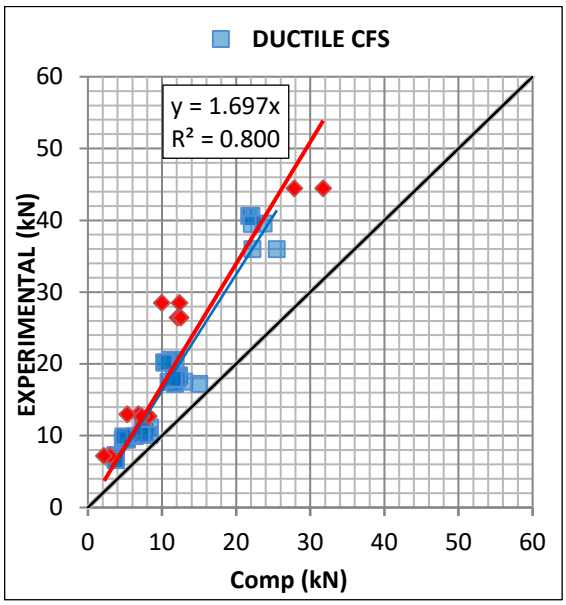

Fig.10 Modified strengths for brittle CFS

4. CONCLUSIONS

Experimental, computational, and numerical evaluation of the flexural strength of C-section CFS were conducted. Based on the results, the following may be concluded.

In terms of failure mode, the majority of the experimental failure modes agreed with computational failure modes. For the ductile CFS, 86.11% of its failure mode in the computation agrees with the experiment, while 75.0% for the brittle CFS. The computation based on NSCP resulted only to distortional bucking. However, when the specimen becomes longer, LTB is observed in the experimental test, especially when the length becomes longer.

FEM analysis was also done to compare further the results attained in the experiment and computations. The FEM and experimental strengths showed good agreement, such that it may be said that the FEM verified the experimental results.

Furthermore, the average ratio between the experimental and computational results was 1.66 for ductile CFS and 1.29 for brittle CFS. Based on these results, it may be concluded that the computed flexural strength based on NSCP is conservative.

Lastly, a modification factor of 0.60 is recommended to be applied to the computation of the strength of brittle CFS. With this, the brittle CFS will have almost the same factor of safety that the ductile CFS has.

5. ACKNOWLEDGMENTS

The authors would like to acknowledge De La Salle University-Manila for providing the testing lab and equipment used for the study. Most of all, this research would not have been possible without the help of our family, mentors, and colleagues. They are truly appreciated for their guidance and assistance for the completion of the study.

6. REFERENCES

[1] Yu W.W., Cold-Formed Steel Design, John Wiley & Sons, Inc., 3rd ed., 2000, pp. 2-3.

[2] Association of Structural Engineers of the Philippines, Inc. (ASEP), National Structural Code of the Philippines, 7th ed., Vol. 1, 2015, pp. 228-279.

[3] Yu A. and Lejano B., "Investigation on the Strength of Cold-Formed Steel C-Section in Compression" in International Conference on Advances on Civil, Structural, Environmental and Bio-Technology CSEB 2014, Kuala Lumpur, Malaysia, 2014.

[4] De Jesus J.M. and Lejano B.A., An Investigation on the Strength of Axially Loaded Cold-Formed Steel Z-Sections. International Journal of GEOMATE, Vol. 14, Issue 42, 2018, pp. 30-36.

[5] American Society for Testing and Materials (ASTM), ASTM E8: Standard Test Methods for Tension Testing of Metallic Materials, 2010.

[6] Wang, L., and Young, B., Design of Cold-Formed Steel Channels with Stiffened Webs Subjected to Bending. Thin-Walled Structures, December 2014, pp. 81-92.

[7] Yu, C. and Schafer, B.W., Distortional Buckling of Cold-Formed Steel Members in Bending. Final Report, Maryland, 2005, pp. 9-14.

[8] Cortese, S.D., Investigation of Single Span Z-Section Purlins supporting Standing Seam Roof Systems considering Distortional Buckling, Master's Thesis, Virginia Polytechnic Institute and State University, Civil Engineering, Virginia, 2001, pp. 8-14.

[9] Chu, X., Kettle, R., and Li, L., Lateral Torsion Buckling Analysis of Partial-Laterally Restrained Thin-Walled Channel-Section Beams, Journal of Construction Steel Research, 2004, pp. 1159-1175.

[10] ANSYS® Academic Research Mechanical, Release 19.0, Help System, Coupled Field Analysis Guide, ANSYS, Inc., 2018.